

Universality of Modified Pattern Decomposition Method for Satellite Sensors

Lifu Zhang^{*}, Yasuko Mitsushita^{**}, Shinobu Furumi^{**}, Kanako Muramatsu^{**},
Noboru Fujiwara^{**}, Motomasa Daigo^{***}
and Liangpei Zhang^{*}

^{*} National Key Laboratory for Information Engineering in Surveying, Mapping, and Remote Sensing, Wuhan University, 129 Luoyu Road, Wuhan 430079, P. R. China

^{**} Laboratory of Nature Information Science, Department of Information and Computer Sciences, Nara Women's University, Nara, Japan

^{***} Department of Economics, Doshisha University, Kyoto, Japan

ABSTRACT

Many kinds of satellite sensors are available for analyzing land cover or net primary production. Unfortunately, the results depend on sensor performance and especially on the number of bands and the wavelength observed, inter-sensor comparisons are difficult. The pattern decomposition method (PDM) is a type of spectral mixing analysis in which each pixel is expressed as the linear sum of fixed three standard spectral patterns: water, vegetation and soil, with supplementary pattern, included when necessary. These standard patterns are calculated from the same original reflectance spectra by each sensor. The same framework can be used to apply PDM to any optical sensor. However, even though standard patterns for n -bands are prepared for each sensor, pattern decomposition coefficients obtained differ for each sensor, even for the sample object.

In this paper, a modified PDM is developed as a universal method of analysis. By this method, the fixed multi-band (92 bands) spectra (four vectors in 92-dimensional space) are used for any sensor as the universal standard spectral patterns. The resulting pattern decomposition coefficients show universality. Estimation errors for pattern decomposition coefficients depend on the sensors. Namely, the estimation errors for Landsat/MSS and ALOS/AVNIR-2 are larger than those Terra/MODIS or ADEOS-II/GLI.

KEY WORDS: RS, Hyper-Multi-spectral RS, Universal PDM

1 INTRODUCTION

There are many kinds of satellite sensors for land analysis. Recent satellite sensors such as Terra/MODIS and ADEOS-II/GLI provide hyper-multi-spectral data. Unfortunately, the results of analysis depend on the performance of the sensor, especially the number of bands and wavelength observed. It is thus difficult to make universal comparisons of analysis made by different satellite sensors. One universalizing method employs the traditional normalized differential vegetation index (NDVI), but it uses reflectance data from only red and near infrared wavelengths (Nemani *et. al.*, 1993).

The pattern decomposition method (PDM) allows for effective use of multi-spectral data (Fujiwara *et. al.*, 1996; Muramatsu *et. al.*, 2000). The PDM is a type of spectral mixing analysis (Adams *et. al.*, 1995) that expresses each pixel as the linear sum of three fixed standard spectral patterns: water, vegetation and soil. The three patterns are given as nearly orthogonal vectors in multidimensional space, and are extracted from the same common spectra measured on the ground. Using the same framework, the PDM can be applicable to any sensors. In this paper, we expand the PDM to develop a universal method of analysis, namely, to obtain pattern decomposition coefficients of sensor independent.

2 ANALYSIS METHOD

2.1 The universal pattern decomposition method

In the PDM, the set of reflectance (or brightness) data for each pixel observed by a sensor is decomposed into the three standard spectral patterns of water, vegetation and soil. If necessary for more detailed analysis, a supplementary standard spectral pattern can be used. The formulation is as follows (Daigo *et al.*, 2003):

$$A(i) \rightarrow C_w \cdot P_w(i) + C_v \cdot P_v(i) + C_s \cdot P_s(i) + C_d \cdot P_d(i), \quad (1)$$

where $A(i)$ is the reflectances of band i , and $P_w(i)$, $P_v(i)$ and $P_s(i)$ are the standard spectral patterns of water, vegetation and soil. $P_d(i)$ is a supplementary spectral pattern. The residual of the i band's reflectance is defined as follows:

$$R(i) = A(i) - \{C_w \cdot P_w(i) + C_v \cdot P_v(i) + C_s \cdot P_s(i) + C_d \cdot P_d(i)\}. \quad (2)$$

The samples used for the standard spectral patterns are ocean water, overlapping leaves and dry sands. The supplementary pattern is obtained from residual $R(i)$ of Equation (2) for a yellow leaf. The standard spectral patterns are normalized as:

$$\sum_i^N |P_k(i)| = 1, \quad (k = w, v, s, d). \quad (3)$$

Where N is the number of bands of a sensor, the decomposition coefficient C_w , C_v , C_s and the

coefficient for the supplementary pattern C_d are evaluated using the least squares method.

In this PDM, the standard patterns depend on the band wavelengths detected by the sensor and on the number of bands, even though the same continuous spectra serve as the standard spectra. As a result, the values of the pattern decomposition coefficients for the same object depend on the sensor. We have developed a new universal PDM in which the pattern decomposition coefficients in the same four-dimensional space of C_w , C_v , C_s and C_d are obtained. In principle, in a sensor independent method, nearly identical values are obtained for data from the same object, regardless of the sensor.

We define standard spectral patterns as a continuous spectral function and instead of Equation (3), normalize as follows:

$$\int |P_k(x)| dx = \Delta w \quad [\text{nm}], \quad (k = w, v, s, d) \quad (4)$$

where x is wavelength [nm] and Δw is width of integrated wavelength. That is, $P_k(x)$ is defined as the average value of $P_k(x)$, which equal one. The spectral patterns of $P_k(x)$ as a function of x are the same as the spectral patterns of reflectance from standard objects. As solar light is used, the spectral region used for analysis is restricted to area where the atmospheric transmittance is higher than 80%. Other wavelength regions are excluded from Equation (4). Table 1 shows the wavelength regions used for standard spectral patterns.

Table 1 Wavelength regions used in this analysis

1.	371.0 ~ 900.0	nm
2.	991.0 ~ 1100.0	nm
3.	1191.0 ~ 1300.0	nm
4.	1521.0 ~ 1750.0	nm
5.	2081.0 ~ 2360.0	nm

The $P_k(i)$ for each sensor in Equation (1) is defined as follows:

$$P_k(i) = \left[\int_{w_i(i)}^{w_f(i)} P_k(x) dx \right] / \{w_f(i) - w_i(i)\}, \quad (5)$$

where $\{w_f(i) - w_i(i)\}$ is wavelength width of band i of a sensor. The $P_k(i)$ is the value $P_k(x)$ at average wavelength x of band i . The reflectance $A(i)$ in Equation (1) is redefined as follows:

$$A(i) \rightarrow A(i) * \Delta w. \quad (6)$$

The pattern decomposition coefficients of Equation (1) are evaluated using the least squares method. The obtained coefficients are values in the same four-dimensional C_k ($k=1,2,3,4$) space. In principle, for datum from the same object, almost the same values are expected for all sensors. In

practice, the precision of the coefficients improves as the number of bands increases.

The fitted reflectance is the value of the right side of Equation (1) divided by Δw . The reduced χ^2 are defined as follows for a sensor of number of bands:

$$\chi^2 = \sum_i r(i)^2 / (n - 4). \quad (7)$$

where $r(i) = R(i) / \Delta w$ and $(n - 4)$ represent the degree of freedom for a dataset of n -bands.

2.2 Standard spectral pattern and sample data

The sample data used in this analysis were measured outdoors under solar light or indoors under a halogen lamp with a Field Spec FR (Analytical Spectral Devices Inc.) or MSR7000 (Opto Research Corp.) radio-spectrometer. Both radio-spectrometers give raw spectral values every 1 nm for wavelength of 350 nm to 2,500 nm. Spectral resolution ranges from 3 to 10 nm. The samples used for standard spectral patterns were the same as those used for reference (Daigo *et. al.*, 2003). Figure 1 shows the new normalized standard spectral patterns of water (blue +), vegetation (green □), soil (red ◇) and the supplement (purple ×). As mentioned in Section 2, the spectral region used for analysis was restricted to where the atmospheric transmittance was higher than 80%.

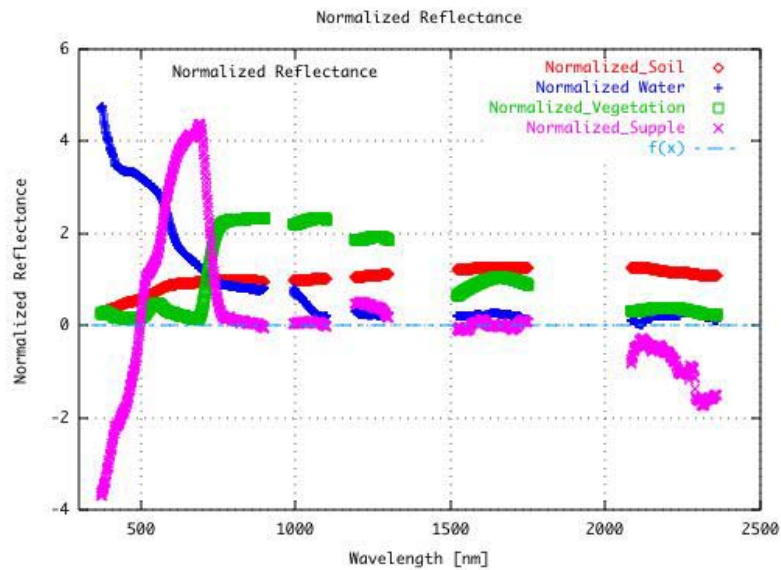


Figure 1. Normalized standard patterns of soil, water, vegetation and the supplementary pattern.

2.3 Sensor and sample data used for analysis

The test sensors (number of bands) used for this analysis were MSS, ALOS, TM, MODIS and

GLI. In addition to these sensors, the model sensors MODEL and CONTINUE (92 bands) were also used. Bands in which output signals from the sensor (MODIS & GLI) were saturated on land areas were removed. In the wavelength region above 2,000 nm, ground-measured data are of poor quality, these data were also removed from this analysis. For each band of each sensor, average reflectance values were obtained from ground-measured data within wavelength width of each band of the sensor. Table 2 lists the bands used in this analysis. The model sensor CONTINUE has 92 bands from wavelength of 371 nm to 1,750 nm as shown in Table 1 with band width of 10 nm.

Table 2 Spectral bands used in this analysis

MSS (4 bands)	ALOS (4 bands)	ETM+(5 bands)	MODIS (6 bands)
499.5 ~ 600.5	420.0 ~ 500.0	449.5 ~ 519.5	459.0 ~ 479.0
599.5 ~ 700.5	520.0 ~ 600.0	519.5 ~ 600.5	545.0 ~ 565.0
699.5 ~ 800.5	610.0 ~ 690.0	629.5 ~ 690.5	620.0 ~ 670.0
799.5 ~ 1,100.5	760.0 ~ 890.0	759.5 ~ 900.5	841.0 ~ 876.0
		1,549.5 ~ 1,750.5	1,230.0 ~ 1,250.0
			1,628.0 ~ 1,652.0
GLI (10 bands)		MODEL (12 bands)	
375.0 ~ 385.0	855.0 ~ 875.0	385.0 ~ 425.0	855.0 ~ 875.0
455.0 ~ 465.0	1,040.0 ~ 1,060.0	455.0 ~ 465.0	991.0 ~ 1,010.0
540.0 ~ 550.0	1,230.0 ~ 1,250.0	540.0 ~ 550.0	1,040.0 ~ 1,060.0
673.0 ~ 683.0	1,540.0 ~ 1,740.0	673.0 ~ 683.0	1,200.0 ~ 1,250.0
705.0 ~ 715.0		705.0 ~ 715.0	1,540.0 ~ 1,640.0
759.0 ~ 767.0		759.0 ~ 767.0	1,650.0 ~ 1,740.0

3 RESULTS AND DISCUSSION

3.1 Reproducibility of observed spectra with universal PDM and reduced χ^2

Figure 2 shows typical original reflectance spectra measured on the ground and the reconstructed reflectance spectra of 92 bands full spectra calculated by the pattern decomposition coefficients obtained for each sensor. In the Figure, red rhombuses shows original measured data. The blue broken line, green broken line and purple crosses represent reconstructed spectra for the ALOS, GLI and CONTINUE sensors. The original spectra are reproduced well except those from ALOS. The reconstructed spectra for TM, MODIS and MODEL are nearly the same as the spectra for GLI and

CONYINUE. The reconstructed spectra for MSS are not shown in the figure. The data points corresponding to wavelengths of the MSS bands (499.5~1,100.5 nm) are exactly reproduced. However, especially above wavelengths of 1,000 nm, the reproduced values differ completely from the original data.

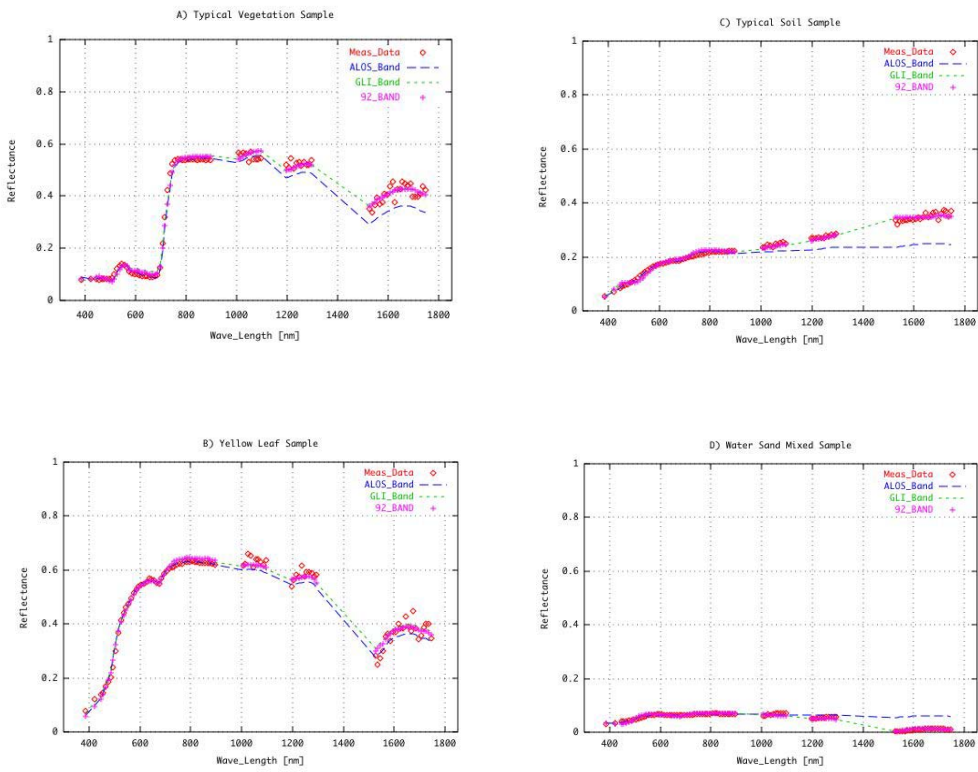


Figure 2. The original reflectance spectra and reconstructed reflectance spectra

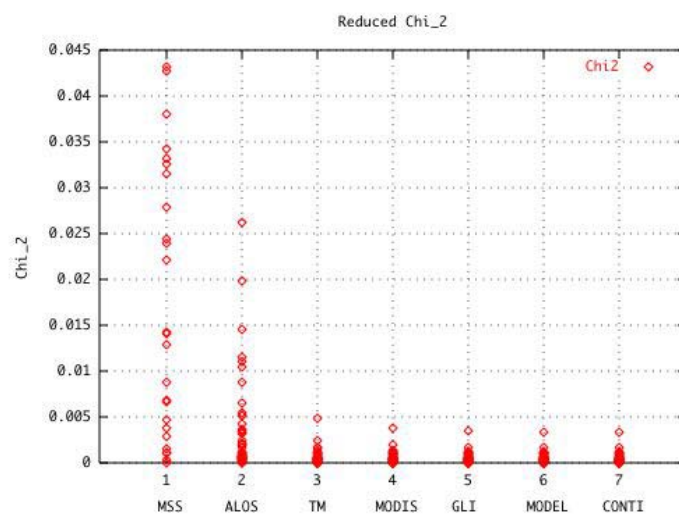


Figure 3. Reduced- χ^2 for reconstructed spectra

Because we have four fitting parameters C_w , C_v , C_s and C_d , the fitting errors for the four-bands sensor (MSS and ALOS) are zero. Figure 3 shows scatter plots of the reduced- χ^2 for the universal PDMs as a function of the sensor. The number of samples is about 1,300. The values decrease according to increases in the band number and converge at 0.00046 for band number larger than five (TM). Table 3 lists the average values of the reduced- χ^2 for each sensor are listed in Table 3. The square root of 0.00032 is 0.018 (1.8%) and is the fitting error per degree of freedom.

Table 3 The average values of reduced- χ^2

MSS	ALOS	ETM	MODIS	GLI	MODEL	CONTINUE
0.11132	0.01117	0.00041	0.00036	0.00038	0.00035	0.00032

3.2 Correlating the pattern decomposition coefficient with the universal PDM

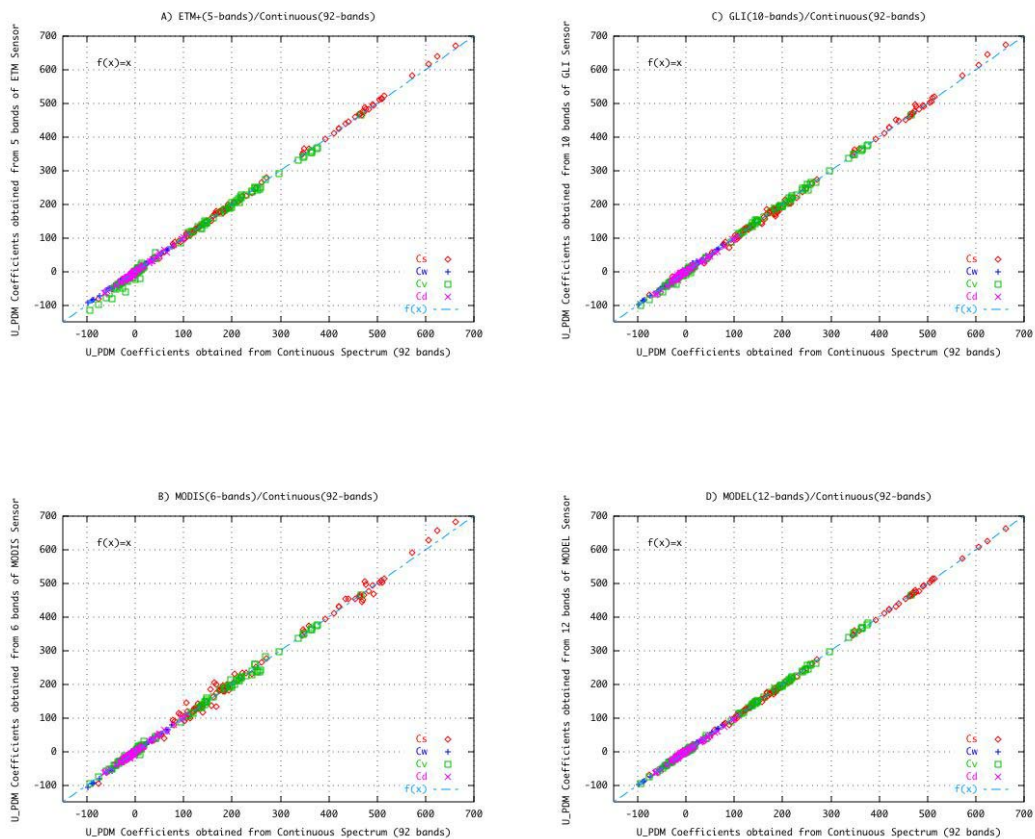


Figure 4. Correlation of universal pattern decomposition coefficients

Figure 4 shows the correlation of the PDM coefficients with the universal pattern decomposition method. The x -axis shows the PDM coefficient for continuous spectra, and the y -axis shows ETM, MODIS, GLI or MODEL sensors. As expected, the coefficients obtained for each sensor are nearly equal to the coefficients obtained from the continuous spectra. This means that the coefficients of the universal PDM are sensor-independent values.

4 SUMMARY AND CONCLUSIONS

We developed a universal pattern decomposition method to obtain sensor-independent pattern decomposition coefficients for reflectance data in the 371nm to 1,750nm wavelength range. We verified that the pattern decomposition coefficients obtained are almost sensor independent, except for four-band sensors such as MSS and ALOS. Using this method, we can sensor-independently analyze satellite data and compare analysis results for land under conditions that effectively reflect multispectral data.

ACKNOWLEDGEMENTS

This work was supported under the ADEOS-II/GLI project by the National Space Development Agency of Japan (NASDA).

REFERENCES

- Nemani, R., Pierce, L., Running, S., and Band, L. (1993). "Forest ecosystem processes at the watershed scale: sensitivity to remotely-sensed leaf area index estimates", *International Journal of Remote Sensing*, 14, 2519.
- Adams, J. B., Sabol, D. E., Kapos, V., Filho, R. A., Roberts, D. A., Smith, M. O., and Gillespie, A. R. (1995). "Classification of multispectral images based on fractions of endmembers: application to land-cover change in the Brazilian Amazon", *Remote Sensing of Environment*, 52, 137-154.
- Daigo, M., Ono, A., Fujiwara, N., and Urabe, R. (2003). "Pattern decomposition method for hyper-multi-spectral data analysis", in printed in *International Journal of Remote Sensing*
- Fujiwara, N., Muramatsu, K., Awa, S., Hazumi, A. and Ochiai, F. (1996). "Pattern expansion method for satellite data analysis", (in Japanese). *Journal of Remote Sensing Society of Japan*, 17(3), 17-37.
- Muramatsu, K., Furumi, S., Fujiwara, N., Hayashi, A., Daigo, M., and Ochiai, F. (2000). "Pattern decomposition method in the albedo space for Landsat TM and MSS data analysis", *International Journal of Remote Sensing*, 21(1), 99-119.